

Electron Spin-Lattice Relaxation of the $[\text{Cu}(1.5) \dots \text{Cu}(1.5)]$ Dinuclear Copper Center in Nitrous Oxide Reductase

Susanne Pfenninger,* W. E. Antholine,* M. E. Barr,[‡] James S. Hyde,* P. M. H. Kroneck,[§] and W. G. Zumft^{||}

*Biophysics Research Institute, Medical College of Wisconsin, Milwaukee, Wisconsin, USA; [‡]Advanced Technology Group, Nuclear Materials Technology Division, Los Alamos National Laboratory, Los Alamos, New Mexico, USA; [§]Fakultät für Biologie, Universität Konstanz, D-78434 Konstanz, Germany; and ^{||}Lehrstuhl für Mikrobiologie, Universität Fridericiana, D-76128 Karlsruhe, Germany

ABSTRACT Relaxation times have been obtained with time-domain EPR for the dinuclear mixed valence $[\text{Cu}_A(1.5) \dots \text{Cu}_A(1.5)]$ $S = 1/2$ center in nitrous oxide reductase, N_2OR , from *Pseudomonas stutzeri*, in the TN5 mutant defective in copper chromophore biosynthesis, in a synthetic mixed valence complex, and in type 1 and 2 copper complexes. Data confirmed that the intrinsic electron spin-lattice relaxation time, T_1 , for N_2OR in the temperature range of 6–25 K is unusually short for copper centers. At best, a twofold increase of T_1 from g_\perp to g_\parallel was measured. Optimized fits of the saturation-recovery data were obtained using both double-exponential and stretched-exponential functions. The temperature dependence of the spin-lattice relaxation rate of mutant N_2OR is about $T^{5.0}$ with the stretched-exponential model or $T^{3.3}$ and $T^{3.9}$ for the model using the sum of two exponentials. These T_1 s are intrinsic to the mixed valence $[\text{Cu}_A(1.5) \dots \text{Cu}_A(1.5)]$ center, and no interaction of the second copper center in wild-type N_2OR with the $[\text{Cu}_A(1.5) \dots \text{Cu}_A(1.5)]$ center has been observed. The T_1 of the mixed valence center of N_2OR is not only shorter than for monomeric square planar $\text{Cu}(\text{II})$ complexes, but also shorter than for a synthetic mixed valence complex, $\text{Cu}_2\{\text{N}[\text{CH}_2\text{CH}_2\text{NHCH}_2\text{CH}_2\text{NHCH}_2\text{CH}_2]_3\text{N}\}$. The short T_1 is attributed to the vibrational modes of type 1 copper and/or the metal-metal interaction in $[\text{Cu}_A(1.5) \dots \text{Cu}_A(1.5)]$.

INTRODUCTION

Multifrequency electron paramagnetic resonance (EPR) data, especially low-frequency S-band and C-band data, have been used to support our hypothesis that the EPR signals in both nitrous oxide reductase (N_2OR) and cytochrome *c* oxidase (COX) are from dinuclear $[\text{Cu}_A(1.5) \dots \text{Cu}_A(1.5)]$, $S = 1/2$ centers (Antholine et al., 1992; Kroneck et al., 1990). The first evidence that a similar $[\text{Cu}_A(1.5) \dots \text{Cu}_A(1.5)]$ center exists in N_2OR and COX came from electron spin-echo envelope modulation (ESEEM) experiments (Jin et al., 1989). Narrow lines at 1.5, 1.9, and 2.9 MHz and broad lines at 0.8 and 3.8 MHz are remarkably similar to lines from the $[\text{Cu}_A(1.5) \dots \text{Cu}_A(1.5)]$ site in COX. The absorption and resonance Raman excitation profiles of the $[\text{Cu}_A(1.5) \dots \text{Cu}_A(1.5)]$ center in N_2OR and COX are also remarkably similar (Andrew et al., 1994). For example, the intensity of the $\gamma(\text{Cu-S})$ mode denotes significant (Cys) $\text{S} \rightarrow \text{Cu}$ CT character in the 480 nm and 530 nm absorption bands. Nevertheless, to our knowledge, only multifrequency EPR data have been used to characterize the dinuclear site as a mixed valence center.

Steffens et al. (1987, 1993) showed that COX from bovine heart contains 3 Cu, 2 Fe, 1 Zn, and 1 Mg, and COX from *Paracoccus denitrificans* contains 3 Cu and 2 Fe (Buse and Steffens, 1991). Many investigators reported a ratio of

about 2 Cu to 2 Fe, but a recent study suggests that a modification (defect) in the enzyme is responsible for this low ratio (Kelly et al., 1993). A ratio of 3 Cu to 2 Fe is required for $[\text{Cu}_A(1.5) \dots \text{Cu}_A(1.5)]$ and Cu_B in COX. A recent x-ray absorption fine structure (EXAFS) study is consistent with a 2.5 Å copper-copper bond in the $[\text{Cu}_A(1.5) \dots \text{Cu}_A(1.5)]$ center of a water-soluble fragment from subunit II of COX (Blackburn et al., 1994). An ESEEM study had assigned the dicopper site in N_2OR to a $[\text{Cu}_Z \dots \text{Cu}_Z]$ center (Jin et al., 1989) (i.e., the coppers at the catalytic site). However, our work (Antholine et al., 1992) with the mutant form of N_2OR (which lacks the $[\text{Cu}_Z \dots \text{Cu}_Z]$ center) suggests that the ESEEM data are for the dinuclear $[\text{Cu}_A(1.5) \dots \text{Cu}_A(1.5)]$ center (see Fig. 1), which is similar to the $[\text{Cu}_A(1.5) \dots \text{Cu}_A(1.5)]$ center in COX and not the $[\text{Cu}_Z \dots \text{Cu}_Z]$ site. An EPR signal for $[\text{Cu}_Z \dots \text{Cu}_Z]$ is observed upon two-electron reduction of N_2OR (Coyle et al., 1985; Farrar et al., 1991). Twenty-five percent of the copper in N_2OR , assuming eight coppers per dimer, is present at $S = 1/2$ as measured using a SQUID susceptometer (Dooley et al., 1991). The 25% reflects the contribution expected for a monomer. A dinuclear $[\text{Cu}_A(1.5) \dots \text{Cu}_A(1.5)]$ center accounts for 50% of the copper. If the remaining copper is antiferromagnetically coupled, a $[\text{Cu}_Z(2+) \dots \text{Cu}_Z(2+)]$ center, the splitting between the singlet and triplet states was estimated to be 200 cm^{-1} (Dooley et al., 1991).

von Wachenfeldt et al. (1994) obtained a fragment of COX without the EPR detectable heme_a. Four lines (38 G separation) of a seven-line pattern are clearly resolved. In an earlier report by us, the heme signal from *ba*₃ COX was broadened at 100 K, although the dinuclear copper signal had four or five lines of the seven-line pattern resolved with

Received for publication 18 January 1995 and in final form 18 August 1995.

Address reprint requests to Dr. William E. Antholine, Biophysics Research Institute, Medical College of Wisconsin, 8701 Watertown Plank Road, Milwaukee, WI 53226. Tel.: 414-456-4032; Fax: 414-266-8515; E-mail: wantholi@post.its.mcw.edu.

© 1995 by the Biophysical Society

0006-3495/95/12/2761/09 \$2.00

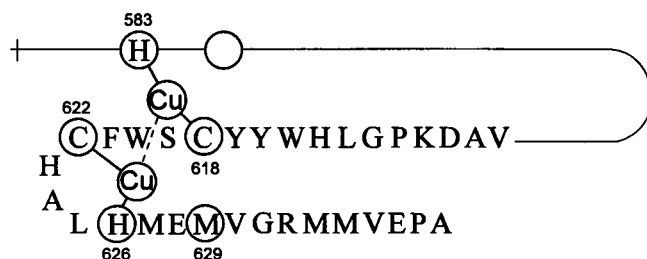


FIGURE 1 A center drawn with an 8-residue loop (629–622), sequence numbers from *P. stutzeri* (Zumft et al., 1992). Lines (—) are used for β sheets, which, other than by analogy to type 1 Cu, are speculative. Bonds for two type 1 copper centers, Cu(His, Cys), are indicated by the short solid lines. Axial ligands, from a methionine and an unknown residue, are speculative. (Note: the two copper atoms are now known to be bridged by two sulfur atoms from cysteines for $[\text{Cu}_A(1.5) \dots \text{Cu}_A(1.5)]$ in COX (Tsukihara et al., 1995; Iwata et al., 1995).)

a 30 G splitting (Kroneck et al., 1993). Recent electron-nuclear double resonance (ENDOR) data confirmed that the hyperfine coupling in beef heart COX is 38 G and 30 G in ba_3 COX (Gurbiel et al., 1993). The overall linewidth of the g_{\parallel} feature in both ba_3 and beef heart COX is consistent with a seven-line pattern. The ENDOR data also reveal nitrogen hyperfine couplings, which are consistent with a $[\text{Cu}_A(1.5) \dots \text{Cu}_A(1.5)]$ center. Although Gurbiel et al. (1993) suggested that the small coupling values, $\sim 3/5$ of the value for a “blue” type 1 cupric site, are due to delocalization onto a second cysteine, such a small nitrogen coupling can also be explained by delocalization of the unpaired electron onto a second copper.

Kelly et al. (1993) have used site-directed mutagenesis to engineer a dinuclear purple site. Two cysteines, two histidines, and one methionine are required for the dinuclear purple copper center (Fig. 1). Thus, relatively few donor atoms are required to construct the purple center. Because the Cu atoms must be in approximately equivalent sites to give an electron-delocalized configuration, two general models have been hypothesized. One model has the two copper atoms with electron transfer occurring via one or more bridging ligands (Antholine et al., 1992; Farrar et al., 1991). This has not been supported by EXAFS. The other model has the copper atoms directly bonded without excluding the possibility of bridging ligands (Blackburn et al., 1994). The second model is supported by EXAFS (Blackburn et al., 1994) and EPR results (Antholine et al., 1992; von Wachenfeldt et al., 1994), showing a short 2.5 Å Cu–Cu distance and electron delocalization. Because most of the electron density is expected to be distributed between the two copper atoms and onto coordinated sulfur atoms, inequivalent nitrogens would not significantly alter the effective chemical environment of each copper atom.

One physical property of the $[\text{Cu}_A(1.5) \dots \text{Cu}_A(1.5)]$ site in N_2OR and COX is the unusually fast relaxation. Although the distance between $[\text{Cu}_A(1.5) \dots \text{Cu}_A(1.5)]$ and heme_a is not precisely known, an analysis of the relaxation suggests a distance of about 10–20 Å. Brudvig et al. (1984)

measured the product T_1T_2 in a relaxation study of the $[\text{Cu}_A(1.5) \dots \text{Cu}_A(1.5)]$ center in COX, which at the time was assumed to be a mononuclear Cu site. The product T_1T_2 exhibits a stronger temperature dependence than in any of the type 1 and type 2 cupric sites. The absence of >10 G splittings indicates a distance between heme_a and $[\text{Cu}_A(1.5) \dots \text{Cu}_A(1.5)]$ that is in excess of 13 Å. A comparison of the saturation of the $[\text{Cu}_A(1.5) \dots \text{Cu}_A(1.5)]$ signal in the native and partially reduced CO derivatives of the enzyme is evidence of a magnetic dipolar interaction between the $[\text{Cu}_A(1.5) \dots \text{Cu}_A(1.5)]$ and the heme_a center, which influences the relaxation of the $[\text{Cu}_A(1.5) \dots \text{Cu}_A(1.5)]$ center (Goodman and Leigh, 1985). A magnetic dipolar interaction between either $[\text{Cu}_A(1.5) \dots \text{Cu}_A(1.5)]$ or heme_a and Fe_{a3}^{2+} -NO is consistent with 20 Å between either $[\text{Cu}_A(1.5) \dots \text{Cu}_A(1.5)]$ and the Fe_{a3} -Cu center or heme_a and the Fe_{a3} -Cu center (Brudvig et al., 1984; Scholes et al., 1984). Scholes et al. (1984) have shown the feasibility of using the saturation-recovery method to directly obtain spin-lattice relaxation times (T_1). Furthermore, our multi-quantum work (Mchaourab et al., 1993) gives T_1 values consistent with the values of Scholes et al. (1984).

This saturation-recovery study reports T_1 values that are field dependent. The saturation-recovery data above 9 K cannot be characterized by a single-exponential function. In addition, our sample from the TN5 mutant defective in copper-chromophore biosynthesis did not have a second paramagnetic signal that may interfere with the interpretation. It is demonstrated that the relaxation of the purple, mixed-valence, dinuclear copper center in N_2OR is unusually fast. Knowledge of the intrinsic relaxation is necessary before dipolar interactions between other paramagnetic metal centers or spin labels (slow relaxers) can be considered (Hyde et al., 1979). This study provides an absolute value for the intrinsic spin-lattice relaxation for the fast relaxer, the $[\text{Cu}_A(1.5) \dots \text{Cu}_A(1.5)]$ center, which, after insertion of a spin label, can be used to calculate the distance-dependent relaxation rate of the slow relaxer—the spin label. If the relaxation of both the fast and slow relaxers is known, the distance between the fast and slow relaxer can be determined.

MATERIALS AND METHODS

Samples

Nitrous oxide reductase, N_2OR , from *Pseudomonas stutzeri* (ATCC 14405) and an inactive enzyme form, obtained from the mutant Tn5 strain MK402, were prepared and analyzed according to the methods of Coyle et al. (1985), Riester et al. (1989), and Zumft et al. (1990). The EPR-detectable site is the $[\text{Cu}_A(1.5) \dots \text{Cu}_A(1.5)] S = 1/2$ center (Antholine et al., 1992), whereas the EPR nondetectable site is the antiferromagnetically coupled $[\text{Cu}_2(2+) \dots \text{Cu}_2(2+)]$ center (Farrar et al., 1991). The inactive mutant has two coppers per monomer and exhibits the EPR-detectable $[\text{Cu}_A(1.5) \dots \text{Cu}_A(1.5)]$ signal. In addition, EPR spectra of the active form have an underlying broad, featureless signal. This featureless signal is absent from some of our samples of the mutant form of the enzyme. The mutant form of the enzyme is defective in chromophore biosynthesis (Riester et al., 1989). Bovine heart COX was a gift from G. Steffens and

G. Buse (RWTH, Aachen, Germany). The protein was analyzed for activity, heme content, and content of Cu, Fe, Mg, Zn, P, and S (Steffens et al., 1993). The synthetic mixed-valence complex $[\text{Cu}_2\text{L}]^{3+}$, where $\text{L} = \text{N}[\text{CH}_2\text{CH}_2\text{NHCH}_2\text{CH}_2\text{NHCH}_2\text{CH}_2\text{N}]$, was prepared as previously described (Barr et al., 1993). Cupric bleomycin (CuBlm) was prepared by addition of a sub-stoichiometric amount of Cu(II) sulfate to Blenoxane, a gift of Bristol-Myers Co., in phosphate buffer. The pH was 7.0. $\text{CuL}^{'+}$, 2-formylpyridine monothiosemicarbazono Cu(II), was a gift from D. H. Petering (University of Wisconsin-Milwaukee). $\text{CuL}^{'+}$ was dissolved in 25% dimethylsulfoxide (Aldrich).

Instrumentation

EPR spectra were recorded on a Varian Century Series spectrometer (Varian, Palo Alto, CA).

The saturation-recovery experiments were performed on a pulse spectrometer designed and constructed at the National Biomedical ESR Center. A 200 MHz oscillator was used to synchronize two delay generators (Stanford Research Systems, model DG535), a transient recorder (DSP Technologies, 100 MHz, model 2001AS or 200 MHz, model 2301), a bi-phase modulator (50 Hz), and a magnetic field modulator (25 Hz). Output from the delay generators was used to control the microwave pump pulse, observer disable, and trigger for the transient recorder. The averager (DSP model 4101) supports both addition and subtraction modes that, when synchronized with the field modulation, allow baseline corrections and improve the suppression of switching transients by automated subtraction of "on" and "off" resonance signals. The averager can accumulate 65,000 transients before it is necessary to transfer data to a PC. The amplitude of the field modulation is limited to about 10 G. Because the linewidths were more than 10 G for all copper sites, data were first collected on-resonance and transferred to the PC. The magnetic field was then manually adjusted to be off-resonance, and the collected data were transferred to the PC to be subtracted from the on-resonance data. Fits for these saturation-recovery signals gave T_1 values. T_1 values from three or more measurements were averaged at each temperature to obtain mean values.

The measurements were performed with a rectangular TE₁₀₂ cavity from Varian. A water warming jacket was used to keep the cavity at a constant temperature. Sample temperatures were controlled by a Heli-Tran flow system (Allentown, PA) comprising a transfer line and digital indicator/controller and a quartz insert dewar. GaAlAs diodes (TG-120-PL) from LakeShore (Westerville, OH) were used to monitor the temperature. Diodes were placed inside the EPR tube just above the sample and outside the EPR tube just below the sample. The gradient between the diodes was less than 1 K, and only the diode at the bottom of the tube was used to determine the temperature of the sample. Experimental conditions for all samples were: microwave frequency, X-band (9 GHz); pump pulse width, 200 μs ; pump power, 125 mW; observe power, 1.2 μW ; trigger delay after the pump pulse, 4 μs .

Analysis

Fits of the saturation-recovery signal to a sum of exponentials were done with a program written by S. Eaton and G. Eaton of the University of Denver, using the method of Provencher (1976). The method is suitable for data composed of random noise, one unknown constant, and a sum of up to five exponential-decay functions. Most probable solutions are estimated from the program itself. Fits of stretched-exponential functions to the saturation-recovery signal have been done with the least-square fitting method of Levenberg-Marquart. The program described in the *Numerical Recipes* (Press et al., 1989) has been translated using Mathematica (Wolfram, 1991), version 2.2, on a Macintosh computer. The two programs gave identical results for exponential fitting functions. The fits to the data points in Figs. 4 and 6 were obtained by linear regression using Grapher for Windows (Golden Software, Inc.). The range for the coefficients of determination, R-squared, is 0.95 to 0.99.

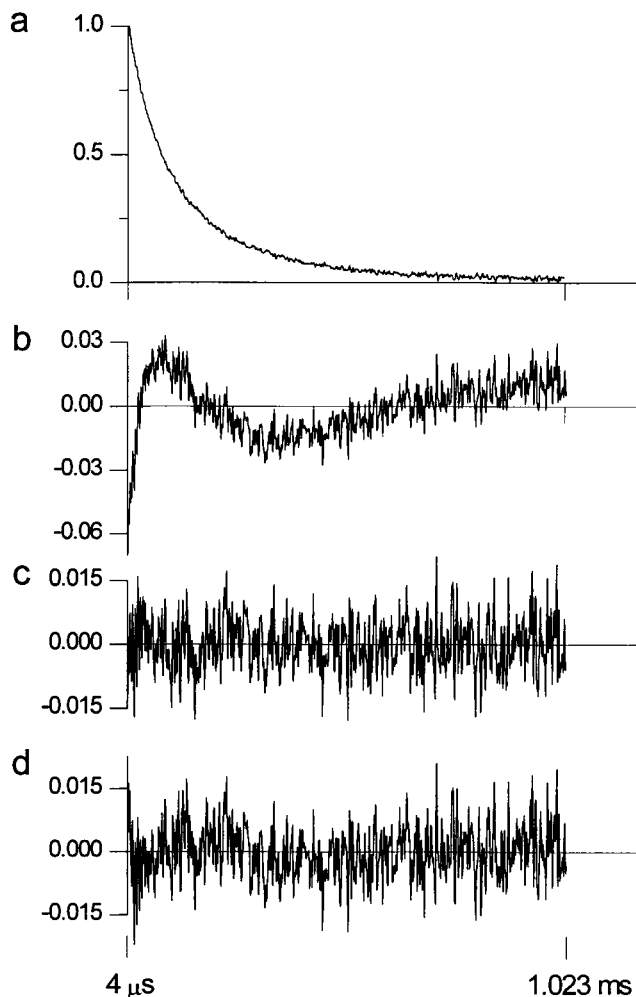


FIGURE 2 Saturation-recovery data (a) for $[\text{Cu}(1.5) \dots \text{Cu}(1.5)] S = 1/2$ site in N₂OR at 9.8 K and an observe power of 1.2 μW . Relative intensity versus time (ms). Spectrometer conditions: pulse width, 200 μs ; TE₁₀₂ cavity; sample interval, 1 μs ; data points, 1024; 32,000 averages. Residual curves from a single-exponential fit (b), $T_1 = 129 \mu\text{s}$, a double-exponential fit (c) $T_{1S} = 62 \mu\text{s}$ and $T_{1\epsilon} = 192 \mu\text{s}$, and a stretched-exponential fit (d) $\alpha = 0.79$ and $T_1 = 109 \mu\text{s}$.

RESULTS

Saturation-recovery signals were collected for the mixed-valence center in N₂OR, which has four coppers per subunit, and for the mutant enzyme, which has up to 3.2 coppers per subunit. The saturation-recovery signals acquired at temperatures above 8 K did not fit well to a single exponential. Better fits were obtained with two exponentials as well as with a stretched exponential fitting function (Koper, 1987, and references therein; Narayanan et al., 1995). Fits to a double exponential suggest the existence of two relaxation mechanisms, whereas a fit to a stretched exponential assumes a single relaxation mechanism with a distribution of spin-lattice relaxation times. The residuals of a single-, double-, or stretched-exponential fit to the saturation-recovery signal are shown in Fig. 2, b–d. The error of the nonlinear least-square fit to the single exponential is 4.5

TABLE 1 Relaxation times for mixed-valence, cupric, and heme complexes

Sample	$T_{1\ell}$ (wt)* (μ s)	T_{1s} (wt)* (μ s)	Temp (K)
Mutant N ₂ OR	43 \pm 6 (.2)	10 \pm 1 (.8)	16
2.5 \times diluted	38 \pm 11	11 \pm 3	16
5 \times diluted	41 \pm 8	11 \pm 2	15
Wild-type (⁶³ Cu) N ₂ OR	41 \pm 5 (.3)	9 \pm 1 (.7)	16
5 \times diluted	40 \pm 4	10 \pm 1	16
Wild-type (^{63/65} Cu) N ₂ OR	47 \pm 4 (.2)	10 \pm 1 (.8)	16
COX	95 \pm 14 (.2)	23 \pm 2 (.8)	16
Mixed valence model complex Cu ₂ L ³⁺ , where L = N[CH ₂ CH ₂ NHCH ₂ CH ₂ NHCH ₂ CH ₂] ₃ N	183 \pm 21 (.7)	50 \pm 5 (.3)	16
CuBlm (i.e., Blm = bleomycin)	550 \pm 10 (.7)	65 \pm 2 (.3)	17
CuL ⁺ , 2-formylpyridine monothiosemicarbazone Cu(II)	320 \pm 20 (.8)	47 \pm 7 (.2)	16
Heme _a from COX	29 \pm 12	7 \pm 2	12
Heme _a from COX	64	18	8.7

* $T_{1\ell}$ is the longer relaxation time, T_{1s} is the shorter relaxation time, and (wt) refers to the weighting factor of exponential decay functions. The number after \pm refers to the standard error of the mean. (Note: the sum of the weighting factors has been normalized to 1 at an instrument deadtime of 4 μ s.)

times higher than the error obtained using a double-exponential model. Equally good fits were obtained assuming a stretched exponential. It has the form

$$I(t) = \exp[-(tT_1^{-1})^\alpha], \quad 0 < \alpha < 1 \quad (1)$$

Here, $\alpha = 1$ corresponds to single-exponential relaxation behavior, and $\alpha < 1$ corresponds to a superposition of subsystems with individual exponential relaxation. The distribution is taken into account by combining the single-exponential decays with a distribution function $S(T_1^{-1})$. That saturation-recovery signal $I(t)$ is given by

$$I(t) = \int_0^\infty e^{-tT_1^{-1}} S(T_1^{-1}) d(T_1^{-1}) \quad (2)$$

T_1 values at the crossover point in the g_\perp region at 16 K were obtained from a double-exponential fit of the saturation-recovery signal for several cupric complexes (Table 1). The numbers in parentheses in Table 1 correspond to the weighting factor for the two exponentials. The larger T_1 is referred to as $T_{1\ell}$ (long), with the smaller T_1 referred to as T_{1s} (short). T_1 values for N₂OR at about 16 K are not as short as those for low spin Fe³⁺ in heme_a. $T_{1\ell}$ and T_{1s} are much shorter for the mixed-valence site in N₂OR than for a type 2, pyramidal, square planar cupric complex CuBlm or the type 2 Cu of CuL⁺ (Table 1).

The [Cu(1.5) . . . Cu(1.5)] center of the wild-type and mutant N₂OR exhibit similar T_1 values, and these are considerably shorter than that observed for the dicopper center of Cu₂L³⁺. Another difference between these [Cu_A(1.5) . . . Cu_A(1.5)] centers is that $g_\perp > g_\parallel$ for Cu₂L³⁺ and $g_\perp < g_\parallel$ for the mixed-valence center in N₂OR. EPR signals are obtained at room temperature for Cu₂L³⁺, CuBlm, and CuL⁺, but not for the mixed-valence site in N₂OR (i.e., presumably because of a very rapid relaxation rate).

The weighting factor at the crossover for the $T_{1\ell}$ decay at 16 K is greater than the weighting for T_{1s} for both type 2 complexes, CuBlm and CuL⁺ (Table 1). The weighting factor at the crossover for T_{1s} at 16 K is greater than the

weighting factor for $T_{1\ell}$ for the mixed-valence centers in N₂OR wild-type, mutant, and COX. In contrast, the weighting factor for $T_{1\ell}$ is greater than the weighting factor for T_{1s} for Cu₂L³⁺, i.e., the weighting factors for Cu₂L³⁺ as well as the T_1 values compare more favorably to type 2 complexes than to the mixed-valence centers in N₂OR and COX, even though Cu₂L³⁺ is a mixed-valence complex.

Assuming that the weights from two exponentials correspond to two states populated by a Boltzmann distribution, a plot of the log of the ratio of weights, i.e., $\log \omega_s/\omega_\ell$, versus $1/T$ gives a measure of the energies for these states. A poorly fit line (not shown), with a coefficient of determination of about 0.7, gives an energy of about 20 cm⁻¹ for the difference in energy between the two excited states. This energy is appropriate for a wobbling motion and not a stretching or bending mode. A wobbling motion is attributed to a low-frequency anharmonic vibration mode (de Abreu et al., 1992). This range of frequencies is consistent with a distribution of frequencies as described by a stretched exponential.

There is, at most, a twofold increase in T_1 from the g_\perp to the g_\parallel region of the [Cu_A(1.5) . . . Cu_A(1.5)] center in N₂OR at 15 K (Fig. 3), and a twofold change in the ratio of the weighting factors; however, the α specified in Eq. [1] is constant. About a twofold increase in T_1 from g_\perp to g_\parallel was observed for CuBlm at 12 K (data not shown). The field dependence of T_1 was first reported by Du et al. (1993) for Cu(Et₂dtc)₂ and for a signal from an irradiated fused-quartz standard (Eaton and Eaton, 1993; Ghim et al., 1995). Metal hyperfine is not the source of the orientation dependence of T_1 for Cu(Et₂dtc)₂, Cu(Et₂dtc)₂ doped in Zn(Et₂dtc)₂, CrO(HEBA)₂, and ⁵³CrO(HEBA)₂ (Du et al., 1993). Furthermore, it is difficult to separate the M_I dependence in mixed-valence complexes. The center line of a seven-line pattern for a mixed-valence complex comprises four $M_I(1)$ $M_I(2)$ components, with $M_I(1):M_I(2)$ equal to $-3/2:+3/2$, $-1/2:+1/2$, $+1/2:-1/2$, and $+3/2:-3/2$. If an M_I dependence exists, an average value would be obtained for the data in Fig. 3.

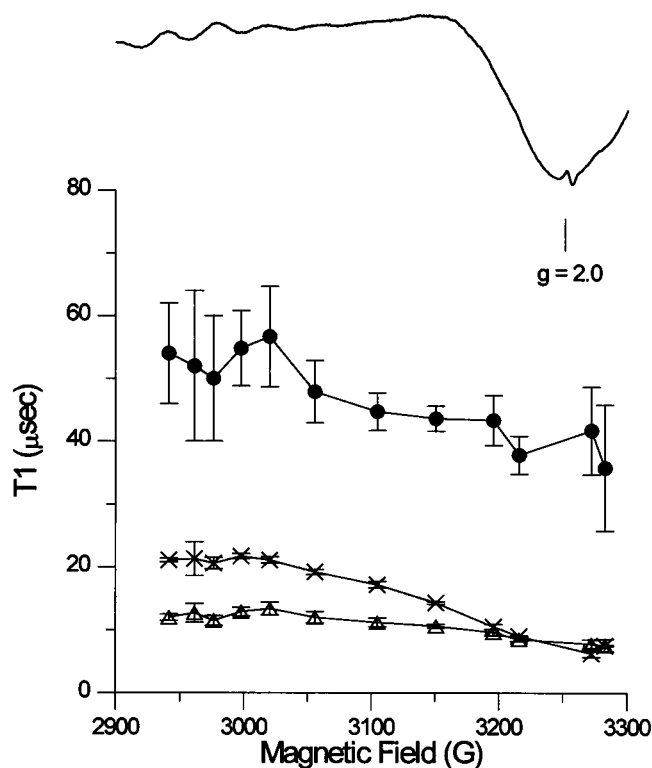


FIGURE 3 Partial EPR spectrum (top) at X-band from the [Cu_A(1.5) ... Cu_A(1.5)] $S = 1/2$ center of wild-type N₂OR. [Note: the radical signal (marked by the line for $g = 2$) was from the quartz insert dewar. Two other dewars used in this work did not have a background signal.] Plot of T_1 (μs) at 15 K versus field from a stretched-exponential fit (x), where α in Eq. 1 is almost independent of the field position (0.64 ± 0.05) and from a double-exponential fit $T_{1\ell}$ (●) and T_{1s} (Δ). Error bars are standard error of the mean.

The EPR signal from the mutant protein is attributed to the mixed-valence [Cu_A(1.5) ... Cu_A(1.5)], $S = 1/2$ site. These EPR data for the mutant confirm that the site that is missing is not the one that gives the EPR signal. Intrinsic relaxation of the mixed-valence site at the crossover has a temperature dependence of $T^{3.3 \pm 0.2}$ for the slower rate and $T^{3.9 \pm 0.3}$ for the faster rate (Fig. 4). Fivefold dilution of the sample has little effect on the relaxation data (Table 1), and therefore, cross-relaxation is not a mechanism. Also, spectral diffusion does not appear to be a mechanism for relaxation under our conditions at 14 K (Fig. 5).

The assignment of forbidden or satellite lines to either T_{1s} or $T_{1\ell}$ could not be achieved under our conditions. Schlick and Kevan (1976) studied ⁶³Cu-doped single crystals. There, the ratio of "apparent" T_1 (forbidden lines), in which ⁶³Cu interacts with matrix protons, to "apparent" T_1 (main lines) is 0.2. But, T_1 values for main lines are actually shorter than those for satellite lines, as determined by the saturation-recovery method for main and satellite lines in irradiated malonic acid (Nechtschein and Hyde, 1970). "Apparent" T_1 values from CW saturation take into account not only the lattice-induced relaxation, but also the microwave-induced transition probability. More power is needed to

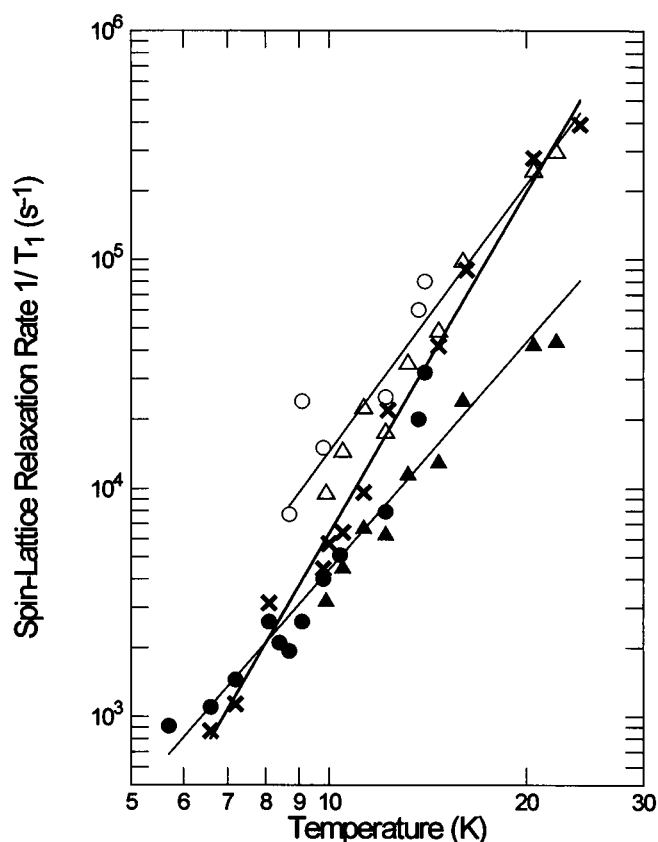


FIGURE 4 Plot of spin-lattice relaxation rate (s^{-1}) versus temperature at the crossover for mutant N₂OR, i.e., only the [Cu_A(1.5) ... Cu_A(1.5)] $S = 1/2$ center. Saturation-recovery data were fit to two exponentials. Filled symbols (●, ▲) indicate the longer T_1 for two independent experiments. Open symbols (○, Δ) indicate the shorter T_1 . Slopes are 3.3 ± 0.2 and 3.9 ± 0.3 , respectively, where the error is the standard error. x, data for the fit of a stretched exponential. The slope of the line through these points is 5.0 ± 0.2 .

saturate the forbidden lines because of the much lower transition probability for the forbidden transition than for the allowed transition, even though T_1 for the forbidden transition may be greater than T_1 for the allowed transition (Nechtschein and Hyde, 1970). Secondary and tertiary transitions can be as intense as the allowed transitions at X-band for cupric complexes (Belford and Duan, 1978). These features depend on the copper-quadrupole interaction, which varies greatly, depending on the ligation. The increase in the intensity of the forbidden lines from the mutant enzyme did not affect the lineshape in the g_{\parallel} region as the microwave power increased (not shown). Also, the weighting factors for $T_{1\ell}$ and T_{1s} in the g_{\perp} region did not change as the pump power was varied from 49 μW to 250 mW. The transition probabilities for the secondary transitions approach zero along the principal axes of the copper g - and A -tensors. But, at least in the g_{\parallel} region of CuBIm or CuL⁺, forbidden or satellite lines are not intense enough to support these mechanisms.

Because no rationale for a second relaxation mechanism seems to exist, saturation-recovery signals were fit to a

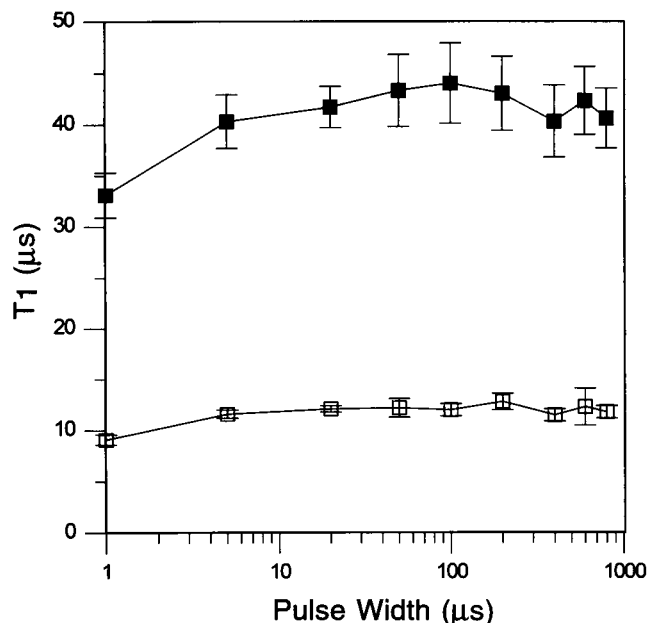


FIGURE 5 Plot of T_1 at the crossover at 14 K for the mutant N_2OR versus pulse width for a double-exponential fit. Upper curve, \blacksquare , T_{1e} ; lower curve, \square , T_{1s} . Error bars are standard error of the mean.

stretched exponential (Fig. 4), where a single relaxation pathway is assumed. The dependence of T_1 on temperature was steeper, i.e., the slope is 5.0 ± 0.2 . The coefficient α in Eq. [1] varied from about 0.8 to 0.5 as the temperature increased from 7 to 20 K. Similarly, the ratio of the weighting for T_{1s} and T_{1e} decreased from 20 to 6 K for the double-exponential fits. Data for T_{1s} below 9 K, where the weighting for T_{1e} was about 10 times greater than the weighting for T_{1s} , are not shown in Fig. 4. Thus, essentially single-exponential fits were obtained for saturation-recovery signals for mutant N_2OR between 5 and 8 K.

When a stretched exponential (or two exponentials) was used to fit the saturation-recovery signals for N_2OR , the data for spin-lattice relaxation rate versus temperature (Fig. 6) were very similar to data for mutant N_2OR (Fig. 4). The slope for the stretched-exponential data (Fig. 6) is 4.8, almost the same as for mutant N_2OR , which is 5.0. Even though N_2OR has 4 Cu/subunit, there is no detectable interaction of the second copper center with the mixed-valence center as determined by the relaxation rate data under the conditions of our experiment. Thus, the T_1 values are intrinsic to the mixed-valence $[Cu_A(1.5) \dots Cu_A(1.5)]$ center.

DISCUSSION

One goal of this work was to make measurements of the electron spin-lattice relaxation times (T_1) of the mixed-valence site in N_2OR using the saturation-recovery method. Single-exponential fits to the saturation-recovery signals were only obtained below 9 K (Fig. 4). Better fits above 8 K were obtained with double-exponential fits and stretched exponentials. Multiexponential fits were necessary not only

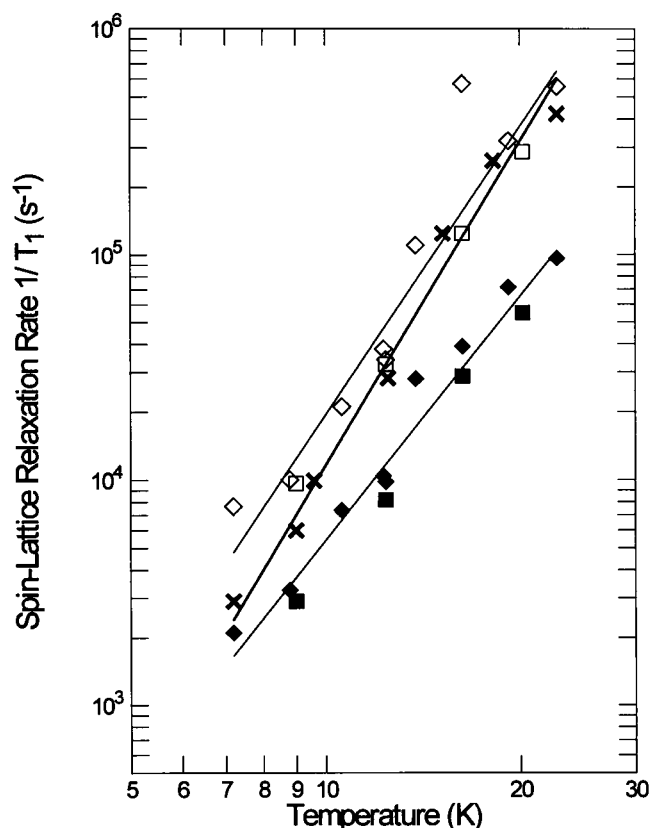


FIGURE 6 Plot of spin-lattice relaxation rate (s^{-1}) versus temperature at the crossover for wild-type N_2OR , i.e., the $[Cu_A(1.5) \dots Cu_A(1.5)]$, $S = 1/2$ center. Saturation-recovery data were fit to two exponentials. Filled symbols (\blacklozenge , \blacksquare) indicate the longer T_1 for two independent experiments. Open symbols (\lozenge , \square) indicate the shorter T_1 . Slopes for the solid lines are 3.6 ± 0.2 and 4.2 ± 0.4 , respectively. \times , data for the fit of a stretched exponential. The slope of the line through these points is 4.8 ± 0.3 .

for the signal of the $[Cu_A(1.5) \dots Cu_A(1.5)]$ center at temperatures above 8 K, but for all saturation-recovery signals from the substances listed in Table 1. Although our data are limited to N_2OR , mutant N_2OR , COX, a synthetic mixed valence complex, two type 2 cupric complexes, and heme_a from cytochrome *c* oxidase, the inability to fit to a single exponential appears to be a general phenomenon and is not peculiar to our studies.

Plots of relaxation rates versus temperature for wild-type N_2OR and mutant N_2OR are similar with respect to absolute values for T_1 . The temperature dependence is $T^{5.0 \pm 0.2}$ for mutant N_2OR and $T^{4.8 \pm 0.3}$ for wild-type N_2OR using a stretched-exponential function. This is excellent agreement for two independent samples in that the relaxation rate for the blue copper protein plastocyanin goes as $T^{4.8}$ to $T^{5.5}$, depending on the preparation of the sample (Drews et al., 1990). Little is known about the EPR-silent copper sites in oxidized N_2OR , but, by analogy to dinuclear sites in other copper proteins, it may be that the EPR-silent copper is due to an antiferromagnetically coupled copper pair in the $S = 0$ state (Farrar et al., 1991). The $S = 1$ state would not be populated under our

conditions. The absence of an enhanced relaxation for the wild-type N₂OR compared with the mutant enzyme is expected if only the $S = 0$ state is populated or if the dipole-dipole distance is great enough to attenuate the dipolar interaction. Thus, the relaxation mechanism is intrinsic to the mixed-valence center in N₂OR.

Makinen and Wells (1987) observed that relaxation is sensitive to isotopic substitution of donor atoms in inner-sphere coordinated ligands. Assuming that vibrations of the ligands contribute to the double- or multi-exponential saturation recovery, T_1 may be sensitive to more vibrational modes in copper complexes as the temperature increases. To a first approximation, the Cu atoms of the dinuclear center are coordinated tetragonally (i.e., $g_{\parallel} > g_{\perp}$). Twice the dinuclear copper hyperfine coupling constant is expected to be about equal to the copper hyperfine coupling constant for a mononuclear Cu(II) complex with comparable ligands. Values of $2 \times 38 \text{ G} \approx 76 \text{ G}$ for A_{\parallel} of N₂OR suggest that the dinuclear site comprises two "blue"-type sites for which $A_{\parallel}^{\text{Cu}}$ is similar to A_{\parallel} of copper in fungal laccase (Reinhammar, 1984). The $[\text{Cu}_A(1.5) \dots \text{Cu}_A(1.5)]$ sites from N₂OR and COX appear to be tetrahedrally distorted type 1 Cu cysteines, as determined from resonance Raman spectra (Andrew et al., 1994). Wobbling modes for the copper-copper center are superimposed on the modes of the blue centers. These modes may be sufficient to explain the fast relaxation. It is argued from CW data that these vibrations are involved in the relaxation mechanism, because the temperature dependence of the relaxation rate for the intrinsic relaxation of the mixed valence site is different than the temperature-dependent relaxation rate for square planar complexes (Brudvig et al., 1984). The temperature-dependent relaxation rate for the dicopper center of Cu_2L^{3+} is more like that of the relaxation rate for square planar complexes. The slower relaxation of Cu_2L^{3+} and square planar complexes may be due to the highly constrained physical environment around the dicopper and monocopper centers. The ligand L, $\text{N}[\text{CH}_2\text{CH}_2\text{NHCH}_2\text{CH}_2\text{NHCH}_2\text{CH}_2]_3\text{N}$, restrains both vibronic and bending modes for the Cu-Cu bond, and this limits the modes of spin-lattice relaxation.

Others have attributed apparent changes in g_{\parallel} or A_{\parallel} for immobilized cupric complexes to a vibronic coupling mechanism, which is effective in type 1 centers, but not in square planar complexes (Bacci and Cannistraro, 1987). The data for N₂OR also fit such a dynamic process. For example, a decrease in α with an increase in temperature may be attributed to an increase in population of more vibrational modes. By comparison, dynamic effects on metallo-cyanide complexes, as measured by temperature-dependent changes in g values, have been attributed to the presence of low-frequency, anharmonic vibration modes of the paramagnetic species (de Abreu et al., 1992, and references therein).

The most important spin-lattice relaxation mechanisms for solids are discussed by Bowman and Kevan (1979). Vibrations in the lattice of ionic solids produce time-

dependent changes in the coupling between the crystal field and orbitals and the spin-orbit coupling. They modulate the hyperfine interaction and the electron field. The relaxation mechanisms associated with rotational oscillations are caused by anisotropic hyperfine interaction or an anisotropic g -tensor. All of these mechanisms might be operative in $[\text{Cu}_A(1.5) \dots \text{Cu}_A(1.5)]$, $S = 1/2$ centers.

The fast relaxation rate for N₂OR (Table 1) and the mutant N₂OR implies the existence of low-lying energy states (Bowman and Kevan, 1979; Piepho, 1990). Formation of a dimer instead of a monomer explains the origin of the low-lying excited states. The 780 nm band of N₂OR from a low-excited state may be attributed to a Cu-Cu intervalence transition in addition to an electronic transition of the Cu-Cys moiety, but no evidence for a Cu-Cu vibration has yet been observed (Andrew et al., 1994).

A comparison of the physical data for mixed-valence centers with the data for type 1 and type 2 cupric sites suggests that T_1 from the $[\text{Cu}(1.5) \dots \text{Cu}(1.5)]$ center reflects the vibrational modes of the type 1 units (Table 2). The seven-line pattern for the copper hyperfine as well as the unusually small hyperfine coupling constant for copper (von Wachenfeldt et al., 1994; Kroneck et al., 1993; Antholine et al., 1992) and superhyperfine values from ENDOR for the nitrogen couplings (Gurbiel et al., 1993) are diagnostic of the sharing of an electron between two cupric ions. As discussed earlier, a doubling of the copper hyperfine and the nitrogen superhyperfine couplings gives values that are consistent with a type 1 configuration. Therefore, both dinuclear centers are distorted type 1 centers. Assuming a Cu-Cu bond, a schematic of the dinuclear site is depicted in Fig. 1. Electron spin echo (ESE) data document the distal nitrogens for the bound histidines (Jin et al., 1989). An analysis of ENDOR data for COX in H₂O or D₂O indicates that H₂O is not bound to $[\text{Cu}_A(1.5) \dots \text{Cu}_A(1.5)]$, whereas analysis of ESE data indicates that the protein-water interface is a minimum of 5.4 Å from the $[\text{Cu}_A(1.5) \dots \text{Cu}_A(1.5)]$ center (Hansen et al., 1993).

Absorbance bands at 480 nm and 780 nm for $[\text{Cu}_A(1.5) \dots \text{Cu}_A(1.5)]$ and 628 nm for azurin are associated with Cu-S charge transfer bands (Andrew et al., 1994). The weak bands at 600 nm in type 2 complexes are assigned to d-d transitions. Strong resonance Raman peaks, including the peak at 347 cm^{-1} of N₂OR and the 340 cm^{-1} peak of COX, also reflect the vibration of the Cu-S bond (Table 2).

The T_1 data in Table 2 are given for a double-exponential model. An intermediate value is obtained for the stretched-exponential model. Values for azurin have been taken from work in progress (McMillin et al., Purdue University), as have values for stellacyanin (C. J. Bender, J. Peisach, G. W. Canters, S. Pfenninger, and W. E. Antholine). Thus, these values reflect the vibrational modes of the type 1 configurations and the dinuclear configuration. These T_1 values agree with data for the electron spin relaxation parameter T_1T_2 , for which the relaxation rates for the $[\text{Cu}_A(1.5) \dots$

TABLE 2 Spectroscopic properties of mixed-valence Cu-Cu centers compared to type 1 and type 2 Cu(II) complexes

		[Cu _A (1.5)...Cu _A (1.5)]					
		COX			Type 1 (distorted trigonal)	Type 2 (square planar)	References
		N ₂ OR	Beef	ba ₃			
EPR hyperfine pattern		7 lines	7 lines	7 lines	4 lines	4 lines	Antholine et al., 1992; von Wachenfeldt et al., 1994
Copper hyperfine couplings		38 G	38 G	30 G	50–90 G 56 G (Az)	140–200 G	Antholine et al., 1992; von Wachenfeldt et al., 1994; Kroneck et al., 1993; Gurbiel et al., 1993
Nitrogen couplings from ENDOR		14 MHz 5 MHz	15.6 MHz 7 MHz	13.8 MHz	27 MHz (Az) 17 MHz	30–45 MHz (Blm)	Gurbiel et al., 1993 and unpublished data for N ₂ OR from Nakagawa, Kroneck, Werst, Hoffman, and Zumft
ESE	Sharp Broad	1.5, 1.9, 2.9 MHz 0.8, 3.8 MHz	1.5, 1.9, 3.2 MHz 0.9, 4.3 MHz		0.8, 1.7, 2.9 MHz 4 MHz	0.5, 1.2, 1.8 MHz 4–5 MHz	Jin et al., 1989; van de Kamp et al., 1993; Burger et al., 1981
T ₁ (16 K)	T _{1e} T _{1s}	43 μs 10 μs	95 μs 23 μs		47 (stella) 30 (Az) μs 9 (stella) 11 (Az) μs	320–560 μs 47–65 μs	This work and unpublished data for Az from McMillin, Pfenninger, Antholine, et al. and for stellacyanin from Bender, Peisach, Canters, Pfenninger, and Antholine
Abs		360 nm 481, 534 nm 630 nm 780 nm	360 nm 480, 530 nm 780 nm		628 nm (strong) (Az)	~600 nm (weak)	Andrew et al., 1994, and refs therein
RR		260, 347 cm ⁻¹ (Cu-S)	258, 340 cm ⁻¹ (Cu-S) 262 cm ⁻¹ (Cu-N)		408, 372, 428 (Cu-S) 285 cm ⁻¹ (Cu-N)		Andrew et al., 1994, and refs. therein

Cu_A(1.5)] center of COX and the type 1 cupric site in azurin, stellacyanin, and plastocyanin have about the same values at 16 K, but the slope of the relaxation parameter for the [Cu_A(1.5) ... Cu_A(1.5)] center versus temperature is sharper for [Cu_A(1.5) ... Cu_A(1.5)] than for the type 1 sites (Brudvig et al., 1984).

In conclusion, it is proposed that the fast relaxation for the [Cu_A(1.5) ... Cu_A(1.5)] center results from low-lying states due to formation of dinuclear copper centers in which each copper has a type 1 configuration. The saturation-recovery signals for the samples in Table 1 fit to a double-exponential function. Cross-correlation, spectral diffusion, and forbidden transitions were considered and dismissed. Unable to find another mechanism, we considered a continuous distribution of local sites. A stretched-exponential function fits as well as the double exponential, but the linkage between Eq. 1 and Eq. 2 is not yet specified, nor are the relaxation mechanism(s). If a single exponential is required, the data are explained in terms of a distribution of local sites. Upon freezing, the distribution might be attributed to a distribution of the ligands, the vibrational states, or wobbling, which are sensitive to temperature. Nevertheless, a double or higher exponential has not been ruled out. Further studies are required to find a physical model for a relaxation mechanism in copper complexes.

The authors thank engineer Theodore Camenisch for providing a state-of-the-art saturation-recovery spectrometer and Joseph Ratke for the software. Dr. Christopher C. Felix was invaluable for the temperature work. Samples of COX from Drs. G. Buse, G. Steffens, and their collaborators are greatly appreciated. The authors also thank Dr. Arthur S. Brill for helpful discussions concerning the population of vibrational states and Drs. Gareth R. and Sandra S. Eaton for referring us to additional significant literature and helpful comments. This work was supported by NSF grant DMB-9105519, National Institutes of Health grants RR01008 and GM27665, and the Deutsche Forschungsgemeinschaft.

REFERENCES

- Andrew, C. R., J. Han, J. deVries, J. van der Oost, B. A. Averill, T. M. Loehr, and J. Sanders-Loehr. 1994. Cu_A of cytochrome *c* oxidase and the A site of N₂OR reductase are tetrahedrally distorted type 1 Cu cysteines. *J. Am. Chem. Soc.* 116:10805–10806.
- Antholine, W. E., D. H. W. Kastrau, G. C. M. Steffens, G. Buse, W. G. Zumft, and P. M. H. Kroneck. 1992. A comparative electron paramagnetic resonance investigation of the multicopper proteins nitrous oxide reductase and cytochrome *c* oxidase. *Eur. J. Biochem.* 209:875–881.
- Bacci, M., and S. Cannistraro. 1987. A vibronic coupling approach for the interpretation of the g-value temperature dependence in type-I copper proteins. *J. Chem. Soc. Faraday Trans. 1*, 83:3693–3700.
- Barr, M. E., P. H. Smith, W. E. Antholine, and B. Spencer. 1993. Crystallographic, spectroscopic and theoretical studies of an electron-delocalized Cu(1.5) ... Cu(1.5) complex. *J. Chem. Soc., Chem. Commun.* 21:1649–52.
- Belford, R. L., and D. C. Duan. 1978. Determination of nuclear quadrupole coupling by simulation of EPR spectra of frozen solutions. *J. Magn. Reson.* 29:293–307.

- Blackburn, N. J., M. E. Barr, W. H. Woodruff, J. van der Oost, S. de Vries. 1994. Metal-metal bonding in biology: EXAFS evidence for a 2.5 Å copper-copper bond in the Cu_A center of cytochrome oxidase. *Biochemistry*. 33:10401–10407.
- Bowman, M. K., and L. Kevan. 1979. Electron spin-lattice relaxation in nonionic solids. In *Time Domain Electron Spin Resonance*. L. Kevan and R. N. Schwartz, editors. John Wiley & Sons, New York. 67–105.
- Brudvig, G. W., D. F. Blair, and S. I. Chan. 1984. Electron spin relaxation of Cu_A and cytochrome *a* in cytochrome *c* oxidase. *J. Biol. Chem.* 259:11001–11009.
- Burger, R. M., A. D. Adler, J. B. Howitz, W. B. Mims, and J. Peisach. 1981. Demonstration of nitrogen coordination in metal-bleomycin complexes by electron spin-echo envelope spectroscopy. *Biochemistry*. 20: 1701–1704.
- Buse, G., and G. C. M. Steffens. 1991. Cytochrome *c* oxidase in *Paracoccus denitrificans*. Protein, chemical, structural and evolutionary aspects. *J. Bioeng. Biomembr.* 23:269–289.
- Coyle, C. L., W. G. Zumft, P. M. H. Kroneck, H. Körner, and W. Jakob. 1985. Nitrous oxide reductase from denitrifying *Pseudomonas perfectomarina*. *Eur. J. Biochem.* 153:459–467.
- de Abreau, C. D., N. M. Pinhal, and N. V. Vugman. 1992. Temperature dependence of *g* values of Fe(I) and Ru(I) cyanide complexes in a KCl host lattice. *J. Magn. Reson.* 100:588–592.
- Dooley, D. M., J. A. Landin, A. C. Rosenzweig, W. G. Zumft, and E. P. Day. 1991. Magnetic properties of *Pseudomonas stutzeri* nitrous oxide reductase. *J. Am. Chem. Soc.* 113:8978–8980.
- Drews, A. R., B. D. Thayer, H. J. Stapleton, G. C. Wagner, G. Giugliarelli, and S. Cannistraro. 1990. Electron spin relaxation measurements on the blue-copper protein plastocyanin. *Biophys. J.* 57:157–162.
- Du, J. L., G. R. Eaton, and S. S. Eaton. 1993. Magnetic field dependence of electron spin-lattice relaxation time. In *The 35th Rocky Mountain Conference on Analytical Chemistry*, Denver, CO. (Abstr.)
- Eaton, S. S., and G. R. Eaton GR. 1993. Irradiated fused-quartz standard sample for time-domain EPR. *J. Magn. Reson.* 102A:354–356.
- Farrar, J. A., A. J. Thomson, M. R. Cheesman, D. M. Dooley, and W. G. Zumft. 1991. A model of the copper centres of nitrous oxide reductase. *FEBS Lett.* 294:11–15.
- Ghim, B. T., S. S. Eaton, G. R. Eaton, R. W. Quine, G. A. Rinard, and S. Pfenninger. 1995. Magnetic field and frequency dependence of electron spin relaxation times of the E' center in irradiated vitreous silica. *J. Magn. Reson.* 115A:230–235.
- Goodman, G., and J. S. Leigh, Jr. 1985. Distance between the visible copper and cytochrome *a* in bovine heart cytochrome oxidase. *Biochemistry*. 24:2310–2317.
- Gurbiel, R. J., Y.-C. Fann, K. K. Surerus, M. M. Werst, S. M. Musser, P. E. Doan, S. I. Chan, J. A. Fee, and B. M. Hoffman. 1993. Detection of two histidyl ligands to Cu_A of cytochrome oxidase by 35 GHz ENDOR: ^{14,15}N and ^{63,65}Cu ENDOR studies of the Cu_A site in bovine heart cytochrome aa₃ and cytochrome caa₃ and ba₃ from *Thermus thermophilus*. *J. Am. Chem. Soc.* 115:10888–10894.
- Hansen, A. P., R. D. Britt, M. P. Klein, C. J. Bender, and G. T. Babcock. 1993. ENDOR and ESEEM studies of cytochrome *c* oxidase: evidence for exchangeable protons at the Cu_A site. *Biochemistry*. 32:13718–13724.
- Hyde, J. S., H. M. Swartz, and W. E. Antholine. 1979. The spin-probe-spin-label method. In *Spin Labeling II. Theory and Applications*. L. J. Berliner, editor. Academic Press, New York. 71–113.
- Iwata, S., C. Ostermeier, B. Ludwig, and H. Michel. 1995. Structure at 2.8 Å resolution of cytochrome *c* oxidase from *Paracoccus denitrificans*. *Nature*. 376:660–669.
- Jin, H., H. Thomann, C. L. Coyle, and W. G. Zumft. 1989. Copper coordination in nitrous oxide reductase from *Pseudomonas stutzeri*. *J. Am. Chem. Soc.* 111:4262–4269.
- Kelly, M., P. Lappalainen, G. Talbo, T. Haltia, J. van der Oost, and M. Saraste. 1993. Two cysteines, two histidines, and one methionine are ligands of a dinuclear purple copper center. *J. Biol. Chem.* 268: 16781–16787.
- Koper, G. J. M. 1987. Relaxation in the random energy model. In *Time Dependent Effects in Disordered Materials*. R. Pynn and T. Rise, editors. Plenum Press, New York. 229–232.
- Kroneck, P. M. H., W. E. Antholine, D. H. W. Kastrau, G. Buse, G. C. M. Steffens, and W. G. Zumft. 1990. Multifrequency electron spin resonance evidence for a bimetallic center in the Cu_A site in cytochrome *c* oxidase. *FEBS Lett.* 268:274–276.
- Kroneck, P. M. H., W. E. Antholine, H. Koteiche, D. H. W. Kastrau, F. Neese, and W. G. Zumft. 1993. The EPR-detectable copper of nitrous oxide reductase as a model for Cu_A in cytochrome *c* oxidase: a multi-frequency electron paramagnetic resonance investigation. In *Bioinorganic Chemistry of Copper*. K. D. Karlin and Z. Tyeklár, editors. Chapman and Hall, New York. 419–426.
- Makinen, M. W., and G. B. Wells. 1987. Application of EPR saturation methods to paramagnetic metal ions in proteins. In *Metal Ions in Biological Systems*, Vol. 22. H. Sigel, editor. Marcel Dekker, New York. 129–206.
- Mchaurab, H. S., S. Pfenninger, W. E. Antholine, C. C. Felix, J. S. Hyde, and P. M. H. Kroneck. 1993. Multiquantum EPR of the mixed valence copper site in nitrous oxide reductase. *Biophys. J.* 64:1576–1579.
- Narayanan, A., J. S. Hartman, and A. D. Bain. 1995. Characterizing nonexponential spin-lattice relaxation in solid-state NMR by fitting to the stretched exponential. *J. Magn. Reson.* 112A:58–65.
- Nechtschein, M., and J. S. Hyde. 1970. Pulsed electron-electron double resonance in an S = 1/2, I = 1/2 system. *Phys. Rev. Lett.* 24:672–674.
- Piepho, S. B. 1990. Vibronic coupling model for the calculation of mixed-valence line shapes: a new look at the Creutz-Taube ion. *J. Am. Chem. Soc.* 112:4197–4206.
- Press, W. H., B. P. Flannery, S. A. Teukolsky, and W. T. Vetterling. 1989. *Numerical Recipes*. Fortran version. Cambridge University Press, New York. 523.
- Provencher, S. W. 1976. An eigenfunction expansion method for the analysis of exponential decay curves. *J. Chem. Phys.* 64:2772–2777.
- Reinhammar, B. 1984. Laccase. In *Copper Proteins and Copper Enzymes*, Vol. III. R. Lontie, editor. CRC Press, Boca Raton, FL. 1–36.
- Riester, J., W. G. Zumft, and P. M. H. Kroneck. 1989. Nitrous oxide reductase from *Pseudomonas stutzeri*: redox properties and spectroscopic characterization of different forms of multicopper enzyme. *Eur. J. Biochem.* 178:751–762.
- Schlick, S., and L. Kevan. 1976. The application of differential saturation to distinguish radial and angular modulation mechanisms of electron spin-lattice relaxation. *J. Magn. Reson.* 22:171–181.
- Scholes, C. P., R. Janakiraman, H. Taylor, and T. E. King. 1984. Temperature dependence of the electron spin-lattice relaxation rate from pulse EPR of Cu_A and heme_a in cytochrome *c* oxidase. *Biochem. J.* 45: 1027–1030.
- Steffens, G. C. M., P. Biewald, and G. Buse. 1987. Cytochrome *c* oxidase is a three-copper, two heme A protein. *Eur. J. Biochem.* 164:295–300.
- Steffens, G. C. M., T. Soulimane, G. Wolff, and G. Buse. 1993. Stoichiometry and redox behavior of metals in cytochrome *c* oxidase. *Eur. J. Biochem.* 213:1149–1157.
- Tsukihara, T., H. Aoyama, E. Yamashita, T. Tomizaki, H. Yamaguchi, K. Shinzawa-Itoh, R. Nakashima, R. Yaono, and S. Yoshikawa. 1995. Structure of metal sites of oxidized bovine heart cytochrome *c* oxidase at 2.8 Å. *Science*. 269:1069–1074.
- van de Kamp, M., G. W. Canters, C. R. Andrew, J. Sanders-Loehr, C. J. Bender, and J. Peisach. 1993. Effect of lysine ionization on the structure and electrochemical behavior of the Met44→Lys mutant of the blue-copper protein azurin. *Eur. J. Biochem.* 218:229–238.
- von Wachenfeldt, C., S. de Vries, and J. van der Oost. 1994. The Cu_A site of the caa₃-type oxidase of *Bacillus subtilis* is a mixed valence binuclear copper center. *FEBS Lett.* 340:109–113.
- Wolfram, S. 1991. *Mathematica: A System for Doing Mathematics by Computer*, 2nd ed. Addison-Wesley, Reading, MA.
- Zumft, W. G., A. Dreusch, S. Löchelt, H. Cuyper, B. Friedrich, and B. Schneider. 1992. Derived amino acid sequences of the nos Z gene (respiratory N₂O reductase) from *Alcaligenes eutrophus* and *Pseudomonas stutzeri* reveal potential copper-binding residues. *Eur. J. Biochem.* 208:31–40.
- Zumft, W. G., A. Viebrock-Sambale, and C. Braun. 1990. Nitrous oxide reductase from denitrifying *Pseudomonas stutzeri* genes for copper-processing and properties of the deduced products, including a new member of the family of ATP/GTP-binding proteins. *Eur. J. Biochem.* 192:591–599.